Journal of Intelligent & Robotic Systems
https://doi.org/10.1007/s10846-018-0922-5

Self-Tuning Time-Energy Optimization for the Trajectory Planning of a Wheeled Mobile Robot

Werther Serralheiro[1] · Newton Maruyama[2] · Fabrício Saggin[3]

Received: 30 November 2017 / Accepted: 16 August 2018

Abstract

In this work a method for trajectory planning based on time-energy optimization of a nonholonomic wheeled mobile robot is proposed. The method utilizes a nonlinear variable change that transforms the nonlinear optimization problem into a discrete second order cone programming that can be solved by convex optimization tools. The formulation of the multiobjective function has two components: the total energy and the traversal time that is weighted by a parameter named penalty coefficient. With the use of the penalty coefficient one can establish a trade-off between the optimization of the total energy and the traversal time. The relation between both objectives draws a Pareto Front in the criterion space parameterized by the penalty coefficient. The rationale of this paper is to assume that the Pareto curve is an exponential function, and to propose an algorithm to estimate its parameters. Using this exponential function it is possible to estimate the Knee Point that is an optimal solution that balances time and energy equally. This systematic approach might be understood as a self-tuning algorithm that estimate the penalty coefficient for the generation of optimal voltage signals. Numerical results illustrate the feasibility of the proposed method.

Keywords Wheeled mobile robot · Trajectory planning · Time-energy optimization · Convex optimization · Pareto optimality

1 Introduction

Energy consumption of robots can oftentimes be minimized during design stage by optimizing the energy efficiency of robot motion systems, such as motors and drivers [1]. Significant results can be also achieved by efficient robot motion planning, which could save battery energy up to 40% [2, 3]. This field of research has recently emerged as an alternative way to improve the energy efficiency of robot motion, and it has not been sufficiently explored.

The term *trajectory planning* is commonly used in the robotics literature to address the problem of determining both the geometric path and the velocity profile of the robot motion. These problems can be solved concomitantly by moving the problem to the configuration space augmented with velocity coordinates. Even though this approach has been proved to be complete [4], it may be computationally impractical since the complexity of planning algorithms usually scales exponentially with the dimension of search space [5].

Therefore, most often the problem is decoupled in two stages. In the first one, a high-level planner computes a collision free geometric path in the robot environment, taking into account task specifications [6]. Once the geometric path is determined by the first stage, a low-level planner defines in the second stage how the robot optimally move along the geometric path based on some optimization criteria while satisfying a set of constraints.

✉ Werther Serralheiro
werther@ifsc.edu.br

Newton Maruyama
maruyama@usp.br

Fabrício Saggin
fabricio.saggin@ec-lyon.fr

[1] Department of Electromechanics, Federal Institute of Santa Catarina, Av XV de Novembro 61, Araranguá, 88905-112, Brasil

[2] Department of Mechatronics Engineering and Mechanical Systems, Polytechnic School of the University of São Paulo, Av. Prof. Mello Moraes, 2231, São Paulo, 05508-030, Brasil

[3] Laboratoire Ampère, Bâtiment H9, Ecole Centrale de Lyon, 36 Av Guy de Collongue, Ecully, 69130, France

Since the mid 80's, the problem of finding a set of valid velocity profiles along the geometric path that stay below maximum values is solved via a re-parameterization of the path by a single variable that represents its normalized length.

Bobrow, Dubowsky and Gibson [7] have presented an algorithm for computing actuator torques that move a manipulator along a predetermined geometric path in minimum time subject to torque constraints. They propose that time-optimal solution is estimated by choosing the velocity profiles as large as possible respecting constraints and controlling via switching curves like bang-bang control.

Pfeiffer and Johanni [8] have proposed to obtain the exact minimum time solution using the geometric properties of a transformed set of dynamic equations. Using Pontryagin's maximum principle optimal smooth velocity profiles can be found using shooting methods [9] or the phase plane method used together with imposed constraints on torque variations [10].

Although the aforementioned approaches have presented important results for the research area their nonconvex formulation do not guarantee the global optimality. Verscheure et al. [11] (see also [12]) present an important transformation that allow to solve the minimum time and/or energy problem of a six degree of freedom robotic manipulator motion along a predefined geometric path using convex optimization tools [13]. Some examples of this approach can be found in the robotics literature [14–16].

Lipp and Boyd [17] uses the Verscheure et al. approach in order to optimize the traversal time of a wide range of vehicles over a fixed geometric path, such as space vehicles, car models and aircrafts. However, underactuated robots had not been considered. Recently, Reynoso-Mora et al. [18] have reformulated the nonlinear dynamic model, considering both Couloumb and viscous frictions. However, this formulation requires a convex relaxation that could not be theoretically proved. Via experimental results authors claim that have not found any counterexample.

Since nonholonomic systems are characterized by kinematic constraints that are not integrable and eliminated from model equations, they bring an extra challenge to the trajectory planning [19]. Serralheiro and Maruyama [20] present a change of variable technique that allows the use of the Verscheure et al. approach in order to optimize the motion of a class of nonholonomic wheeled mobile robots.

The first objective of this work is to present a time-energy optimization for the trajectory planning of a nonholonomic wheeled mobile robot (WMR) model over a fixed geometric path. To this aim, Section 2 presents an alternative generalized coordinate system that is used to reduce the dynamic equations by considering that the fixed geometric path that the robot must traverse is itself a constraint. The minimal time-energy problem is transformed into a discrete Second Order Cone Programming (SOCP) that can be solved by convex optimization tools.

In Section 3 experimental results shows that the formulation gives rise to a Pareto optimality condition from which is not possible to diminish the traversal time without increasing the total energy and vice versa. Experimentally it is shown that this relation between the traversal time and total energy might be described by an exponential function. A particular optimal solution is the Knee Point of this function where time and energy are balanced equally.

A self tunning algorithm is presented in Section 4 that can estimate the Knee Point. Simulation results are discussed in Section 5. Finally in Section 6 some conclusions are drawn about the proposed method.

2 Time-Energy Optimization of a WMR

2.1 Robot Kinematic Model

A differential wheeled mobile robot (WMR) is a chassis with two parallel driven wheels with radii r. The distance between wheels is given by l. Consider the *position* $p \in \mathbb{R}^2$, $p = [\,x \;\; y\,]^T$, the vector representing the cartesian coordinates of the midpoint P between the wheels, and the classical *pose* [19] given by $\xi = [\,p \;\; \theta\,]^T = [\,x \;\; y \;\; \theta\,]^T$, where $\theta \in [0, 2\pi)$ is the robot orientation. Also consider the *path* Γ a C^2 class curve in the configuration space where the robot must traverse.

Lemma 1 *If the robot linear velocity is non-negative, a path Γ described by the robot positions $p(t) = [\,x(t) \;\; y(t)\,]^T$ also defines the robot poses $\xi(t) = [\,x(t) \;\; y(t) \;\; \theta(t)\,]^T$ in the configuration space.*

Proof Since the path is a C^2 class curve, the continuous derivative $\dot{p}(t) = [\,\dot{x}(t) \;\; \dot{y}(t)\,]^T$ exists. The heading angle given by

$$\theta(t) = \tan^{-1}\left(\frac{\dot{y}(t)}{\dot{x}(t)}\right) \tag{1}$$

is a continuous function of $\theta : [0, T_f] \rightarrow [0, 2\pi)$. $\square$

Moreover, consider the monotonically increasing function $\gamma : \mathbb{R} \rightarrow \mathbb{R}$ defined as

$$\gamma(t) = \int_0^t v(\iota)\, d\iota = \int_0^t \sqrt{\dot{x}^2(\iota) + \dot{y}^2(\iota)}\; d\iota, \tag{2}$$

witch represents the distance traversed by the robot along the path Γ.

Lemma 2 *If the robot linear velocity is non-negative, a path Γ described by the robot positions $p(t) = [\,x(t) \;\; y(t)\,]^T$ can* *be equivalent defined by the function* $q(t) : [0, T_f] \to \mathbb{R}^2$, $q(t) = [\,\gamma(t)\;\; \theta(t)\,]^T$, *if the initial position* $p_0 = [\,x_0\;\; y_0\,]^T$ *is known.*

Proof Since the path is a C^2 class curve, the function $\gamma(t) = \gamma(p(t))$ defined in Eq. 2 exists as a continuous function. By the Lemma 1, $\theta(t) = \theta(p(t))$. Hence, $q(t) = q(p(t))$. Moreover, the robot positions can be given by the integrals

$$x(t) = x_0 + \int_0^t \gamma(\iota)\cos\theta(\iota)\;\, d\iota,$$
$$y(t) = y_0 + \int_0^t \gamma(\iota)\sin\theta(\iota)\;\, d\iota. \tag{3}$$

Then, $q(t) = q(p(t))$ and $p(t) = p(q(t))$. □

This formulation provides the dimension reduction of the robot coordinates as the following:

Theorem 1 *The function* $q(t) : [0, T_f] \to \mathbb{R}^2$,

$$q(t) = [\,\gamma(t)\;\; \theta(t)\,]^T, \tag{4}$$

can define a path Γ *in the generalized coordinates way, if the initial position* $p_0 = [\,x_0\;\; y_0\,]^T$ *is known.*

Proof By the Lemma 1, the functions $x(t)$ and $y(t)$ also define the heading angle $\theta(t)$ in a C^2 class curve; since the Γ curve can be represented by both distance and heading angle function (Lemma 2) □

2.2 Robot Dynamic Model

The robot input voltage signals $u \in \mathbb{R}^2$, $u = [\,u_r\;\; u_l\,]^T$ impose torque to the wheels. Given the mass m and the moment of inertia J of the robot structure, consider the simplified robot dynamics written as:

$$\mathbf{R}u = \mathbf{M}\ddot{q}, \tag{5}$$

with matrices defined by:

$$\mathbf{R} = \begin{bmatrix} \frac{K_m}{r} & \frac{K_m}{r} \\ \frac{K_m l}{2r} & -\frac{K_m l}{2r} \end{bmatrix}, \tag{6}$$

$$\mathbf{M} = \begin{bmatrix} m & 0 \\ 0 & J \end{bmatrix}, \tag{7}$$

where K_m is the motor torque constant, and $\ddot{q} \in \mathbb{R}^2$, $\ddot{q} = [\,\ddot{\gamma}\;\; \ddot{\theta}\,]^T$ is the acceleration vector.

2.3 Problem statement

Consider a given path Γ defined mathematically as a function $s : [0, 1] \to \mathbb{R}^2$ such that,

$$q(t) = s(\tau(t)), \quad t \in [0, T_f], \tag{8}$$

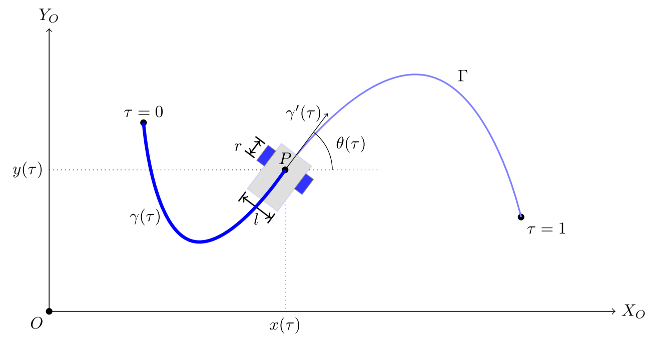

Fig. 1 The WMR and its coordinates in two different representations, traversing a predefined geometric path Γ parameterized by τ

where the robot must traverse a geometric path as illustrated in Fig. 1. The monotonically increasing function $\tau : [0, T_f] \to [0, 1]$ maps the robot motion time in a normalized interval where $\tau(0) = 0$ e $\tau(T_f) = 1$.

The derivatives of Eq. 8 are the robot velocity and acceleration in the configuration space [7]:

$$\dot{q}(t) = s'(\tau)\dot{\tau}(t), \tag{9}$$
$$\ddot{q}(t) = s'(\tau)\ddot{\tau}(t) + s''(\tau)\dot{\tau}^2(t), \tag{10}$$

where $(.)'$ refers to the derivatives with respect to τ.

We want to find a velocity profile $\dot{q}(t)$, $t \in [0, T_f]$, such that the robot is driven through a geometric path s in minimum traversal time T_f and energy consumption E_t. This problem might be defined as an optimization problem that is described as:

Problem 1 *(Minimal time-energy problem)*

$$\underset{(u,\tau)}{min.} : \mathcal{J}(t, u) = \int_0^{T_f} \|u(t)\|_2^2\, dt + \mu \int_0^{T_f} dt, \tag{11}$$
$$s.t. : \mathbf{R}u(t) = \mathbf{M}\ddot{q}(t), \tag{12}$$
$$q(t) = s(\tau(t)), \tag{13}$$
$$u_{min} \le u(t) \le u_{max}, \tag{14}$$
$$\dot{q}_{min} \le \dot{q}(t) \le \dot{q}_{max}, \tag{15}$$
$$\ddot{q}_{min} \le \ddot{q}(t) \le \ddot{q}_{max},\; t \in [0, T_f], \tag{16}$$

where $\mu \in \mathbb{R}$, named *penalty coefficient*, controls the trade-off between time and energy in the objective function. The constants $(u_{min}, u_{max}) \in \mathbb{R}^2$ are the motors input voltage limits, and the pairs $(\dot{q}_{min}, \dot{q}_{max})$, $(\ddot{q}_{min}, \dot{q}_{max}) \in \mathbb{R}^2$ are the limits of the robot velocity and acceleration in the geometric path respectively.

2.4 Convexification

By using Eq. 10 in Eq. 5, that defines the WMR dynamics, yields [11, 17]:

$$\mathbf{R}u(\tau) = \mathbf{M}\left(s'(\tau)\ddot{\tau}(t) + s''(\tau)\dot{\tau}^2(t)\right). \tag{17}$$

Two auxiliary functions are introduced, $a(\tau) = \ddot{\tau}$ and $b(\tau) = \dot{\tau}^2$ which results in the relation $b'(\tau) = 2a(\tau)$. The objective function given by Eq. 11 can be redefined as,

$$\begin{aligned} \mathcal{J}(\tau, u) &= \int_{\tau(0)}^{\tau(T_f)} [\|u(\tau)\|_2^2 + \mu] \tfrac{d\tau}{\dot{\tau}} \\ &= \int_0^1 \tfrac{[\|u(\tau)\|_2^2 + \mu]}{\sqrt{b(\tau)}} \; d\tau, \end{aligned} \tag{18}$$

and the nonlinear Problem 1 becomes equivalent to the following problem:

Problem 2 *(Minimal time-energy convex problem)*

$$\underset{(u,a,b)}{min.} : \mathcal{J}(\tau, u) = \int_0^1 \frac{[\|u(\tau)\|_2^2 + \mu]}{\sqrt{b(\tau)}} \; d\tau, \tag{19}$$

$$s.t. : \mathbf{R}u(\tau) = \mathbf{M}\left(s'(\tau)a(\tau) + s''(\tau)b(\tau)\right), \tag{20}$$

$$b'(\tau) = 2a(\tau), \tag{21}$$

$$(u(\tau), a(\tau), b(\tau)) \in \mathcal{C}_\tau, \; \tau \in [0, 1], \tag{22}$$

where:

$\mathcal{C}_\tau = \{(u(\tau), a(\tau), b(\tau))|$
$(u(\tau), s'^2(\tau)b(\tau), s'(\tau)a(\tau) + s''(\tau)b(\tau)) \in \mathcal{C}_t\}$.

2.5 Convexity Analisys

Since the set $\mathcal{C}_\tau$ is convex and the equality constraints (20) and (21) are affine and linear respectively, the convexity analisys focused on the objective function. Let review the condition:

Theorem 2 (Second-order condition) *The function f is convex if and only if $dom f$ is convex and its Hessian is positive semidefinite, i.e., for all $x \in dom f$, $\nabla^2 f(x) \succeq 0$.* [13]

The Eq. 19 can be written as:

$$\mathcal{J} = \int_0^1 F_1 \; d\tau + \mu \int_0^1 F_2 \; d\tau \tag{23}$$

where $F_1 = b^{-\frac{1}{2}}\|u\|_2^2 = b^{-\frac{1}{2}}u^T u$, $F_2 = b^{-\frac{1}{2}}$, $b = b(\tau)$, $u = u(\tau)$. The function F_2 in on the form x^a, $a \le 0$, hence convex in $\mathbb{R}_{++}$. [13]

Lemma 3 *$F_1 : \mathbb{R}_+ \times \mathbb{R} \to \mathbb{R}$, $F_1 = b^{-\frac{1}{2}}\|u\|_2^2$ is convex in its domain.*

Proof Such $u = u(\tau) = [u_r(\tau) \;\; u_l(\tau)]^T$, consider the notation:

$$\frac{d}{d\tau}\left(u(\tau)^T u(\tau)\right) = 2(u_r(\tau) + u_l(\tau)) = 2\|u(\tau)\|_1. \tag{24}$$

Hence, the Hessian is given by:

$$H = \nabla^2 F_1(b, u) = \begin{bmatrix} \frac{3}{4}b^{-\frac{5}{2}}\|u\|_2^2 & -b^{-\frac{3}{2}}\|u\|_1 \\ -b^{-\frac{3}{2}}\|u\|_1 & 2b^{-\frac{1}{2}} \end{bmatrix}. \tag{25}$$

Let λ_1 and λ_2 be the eigenvalues of H. Such $det(H) = \lambda_1\lambda_2$, $det(H) \ge 0$ implies that all H eigevalues are non-negative. On the other hand, if $det(H)$ is non-negative, than (i) both eigenvalues are positive or (ii) both eigenvalues are negative. Such $trace(H) = \lambda_1 + \lambda_2$, if $det(H) \ge 0$ and $trace(H) \ge 0$, then the eigenvalues are non-negative.

Whereby $b \in \mathbb{R}_+$, $\|u\|_1 \in \Re$, hence:

$$\begin{aligned} det(H) &= \frac{\|u\|_2^2}{2b^3} \ge 0, \\ trace(H) &= \frac{3}{4}b^{-\frac{5}{2}}\|u\|_2^2 + 2b^{-\frac{1}{2}} \ge 0, \end{aligned}$$

then $H = \nabla^2 F_1(b, u) \succeq 0$ which implies $F_1 = b^{-\frac{1}{2}}\|u\|_2^2$ is convex on its domain. □

The Problem 2 is a convex optimization problem, since the objective function (19) is convex, the equality constraints (20) and (21) are afine function of the optimization variables, and $\mathcal{C}_\tau$ is a convex set [13].

2.6 Problem Discretization

Following the approach proposed by Verscheure et al. [11], the time parameter τ is discretized into $N + 1$ points.

Problem 3 *(Discrete minimum time-energy convex problem)*

$$\underset{(u_i,a_i,b_i)}{min.} : \mathcal{J}(\tau, u) = \sum_{i=1}^{N} \frac{2(\|u_i\|_2^2 + \mu)}{\left(\sqrt{b_i} + \sqrt{b_{i-1}}\;\right)}(\delta\tau_i), \tag{26}$$

$$s.t. : \mathbf{R}u_i = \mathbf{M}\left[\bar{s}_i' a_i + \frac{\bar{s}_i''}{2}b_i + \frac{\bar{s}_i''}{2}b_{i-1}\right], \tag{27}$$

$$b_i - b_{i-1} = 2a_i(\delta\tau_i), \tag{28}$$

$$(u_i, a_i, b_i) \in \mathcal{C}_{\bar{\tau}}, \; i = 1, \ldots, N, \tag{29}$$

where:

$\mathcal{C}_{\bar{\tau}} = \{(u_i, a_i, b_i)|$
$(u(\bar{\tau}), s'^2(\bar{\tau})b(\bar{\tau}), s'(\bar{\tau})a(\bar{\tau}) + s''(\bar{\tau})b(\bar{\tau})) \in \mathcal{C}_t\}$,

and $\delta\tau_i = \tau_i - \tau_{i-1}$.

2.7 Formulation as SOCP

Though the Problem 3 is a discrete convex optimization problem, the objective function in Eq. 26 is nonlinear. Therefore, four new scalar variables $c_i, d_i, e_i, f_i \in \mathbb{R}_+$ are introduced in Problem 3 in order to redefine the objective function as:

$$\begin{aligned} \tilde{\mathcal{J}}(\tau, u) &= \sum_{i=1}^{N} 2(e_i + \mu f_i)\delta\tau_i \ge \\ &\ge \sum_{i=1}^{N} \frac{2(\|u_i\|_2^2 + \mu)}{\left(\sqrt{b_i} + \sqrt{b_{i-1}}\;\right)}(\delta\tau_i) = \mathcal{J}(\tau, u), \end{aligned} \tag{30}$$

where the inequality relations:

$$\frac{1}{d_i} \leq f_i, \tag{31}$$
$$\frac{u_i^T u_i}{d_i} \leq e_i, \tag{32}$$
$$d_i \leq c_i + c_{i-1}, \tag{33}$$
$$c_i \leq \sqrt{b_i}, \tag{34}$$

can be considered as constraints which minimize the objective function, i.e., $\tilde{\mathcal{J}} \geq \mathcal{J}$ is an upper constraint bound of $\mathcal{J}$, it means that minimizing $\tilde{\mathcal{J}}$ ensures that $\mathcal{J}$ is minimal. Moreover, $\tilde{\mathcal{J}}$ is a linear function of the new optimization variables. Transforming the hyperbolic inequalities constraints (31), (32) and (34) into second order constraints [21], the Problem 3 becomes equivalent to:

Problem 4 *(Discrete Minimal Time-Energy Convex Problem as a SOCP)*

$$\min_{\left(\substack{u_i \\ a_i,\cdots,f_i}\right)} : \mathcal{J}(\tau, u) = \sum_{i=1}^{N} 2(e_i + \mu f_i)\delta\tau_i, \tag{35}$$
$$s.t. : \left\| \begin{bmatrix} 2 \\ d_i - f_i \end{bmatrix} \right\|_2 \leq d_i + f_i, \tag{36}$$
$$\left\| \begin{bmatrix} 2u_i \\ e_i - d_i \end{bmatrix} \right\|_2 \leq e_i + d_i, \tag{37}$$
$$\left\| \begin{bmatrix} 2c_i \\ b_i - 1 \end{bmatrix} \right\|_2 \leq b_i + 1, \tag{38}$$
$$d_i \leq c_i + c_{i-1}, \tag{39}$$
$$\mathbf{R}u_i = \mathbf{M}\left[\bar{s}_i' a_i + \frac{\bar{s}_i''}{2} b_i + \frac{\bar{s}_i''}{2} b_{i-1}\right], \tag{40}$$
$$b_i - b_{i-1} = 2a_i(\delta\tau_i), \tag{41}$$
$$(u_i, a_i, b_i) \in \mathcal{C}_{\bar{\tau}}, \; i = 1, \ldots, N. \tag{42}$$

Solving the Problem 4, the optimal input signal u_i^* and the optimal auxiliary variables $(a^*, \cdots, f^*)$ are found.

Thereby, the time t can be re-parameterized by the rate: $\delta t_i = \delta\tau_i / \sqrt{b^*(\tau_i)}$, as well as the traversal time and the total energy consumption are calculated by the sums

$$T_f = \sum_{1}^{N} \frac{\delta\tau_i}{\sqrt{b_i^*}}, \tag{43}$$
$$E_t = \sum_{1}^{N} \|u_i^*\|_2^2. \tag{44}$$

3 Experimental Pareto Front

A wheeled mobile robot is considered with the following characteristics: width $B = 0.4m$, inertial mass $m = 10kg$, moment of inertia $J = 2.833Kg/m^2$, wheel radius $r = 0.1m$, motor torque constant $K_m = 65 \cdot 10^{-3} Nm/V$, nominal input voltage $u_{max} = -u_{min} = 12V$.

For instance, the WMR is supposed to traverse the arbitrary geometric path Γ built as a spline with a smoothing parameter value $\varrho = 0.99$ to reach the following waypoints: $p_0 = [0 \;\; 0]^T$, $wp_1 = [2 \; -1]^T$, $wp_2 = [3 \; -1]^T$, $wp_3 = [6 \; -1]^T$, $wp_4 = [8 \; -1]^T$ and $wp_5 = [5 \; -1]^T$.

The spline is then divided into $N = 500$ segments of equal length, resulting in $N + 1$ discrete points $p_0, \ldots, p_N$. as illustrated in Fig. 2.

The robot motion has constraints on maximum velocity $\dot{q}_{max} = [2.5m/s \;\; 1rad/s]^T$ and maximum acceleration $\ddot{q}_{max} = [2m/s^2 \;\; .5rad/s^2]^T$. Furthermore $b_0 = b(\tau_0) = 0$. No final velocity constraint is imposed.

The optimization variables are the left and right motors input voltage $u_i = [u_{ri} \;\; u_{li}]^T$, auxiliary variables a_i and b_i, and also auxiliary variables c_i, d_i, e_i and f_i, $i = 1, \ldots, N$ that are defined by Eqs. 31, 32, 33 and 34. A desktop computer equipped with a 3.60Ghz clock Intel Core i7-4790, 8GB of RAM running Windows 8 x64 is utilized. All numerical calculations are performed by the MATLAB R2017a.

Optimization trials of the Problem 4 have been performed while varying the penalty coefficient μ, using the Mosek algorithm of the MATLAB CVX toolbox [22].

When the penalty coefficient μ decreases towards zero, $\mu \to 0$, the optimization algorithm gradually diminishes the importance of the traversal time T_f while increasing the importance of the total energy E_t. As a consequence, the robot velocity diminishes thus increasing the traversal time T_f. The extreme situation of $\mu = 0$,i.e., only optimization of the total energy E_t is of concern, the traversal time is equivalent to $T_f = 1218s$ while consuming $E_t = 1.4mJ$.

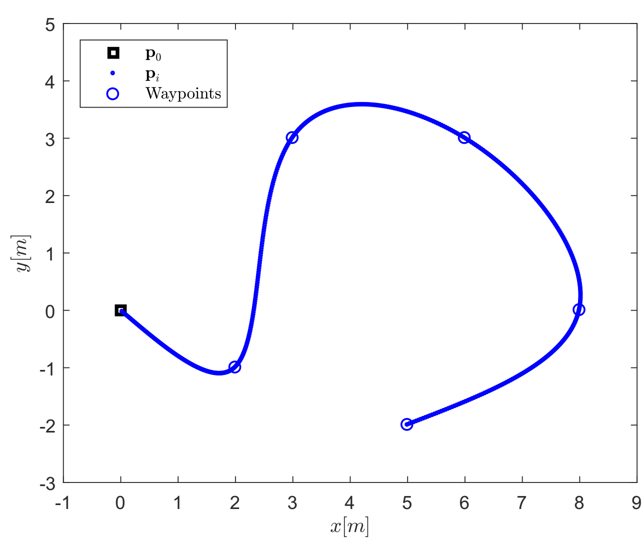

Fig. 2 Arbitrary geometric path Γ in the Cartesian plane. The black squared mark represents the initial point p_0 and the blue dots are the discrete points $p_i, i = 1, \ldots, N$

On the contrary, if only the optimization of the traversal time T_f is important than one can set a very large penalty coefficient $\mu \rightarrow \infty$. In this case, the traversal time is $T_f = 12.8s$ and the energy effort is $E_t = 1704J$.

Figure 3 illustrates a series of optimal input voltage signals (a) u_r^* and (b) u_l^* and the optimal velocity profile (c) v^* while varying the penalty coefficient μ.

The arrows indicates that the higher the value of the penalty coefficient μ, the greater the effort of the motor; consequently, the greater the linear velocity over the geometric path. it is possible to note saturation on input signals (e.g. on u_r^* at $i = 250$ and on u_l^* at $i = 120$) and the linear velocity saturation $v_{max} = 2.5m/s$ on the interval $[285 \leq i \leq 332]$.

In general, there are infinite possible input voltage profiles that can drive the robot through the geometric path Γ, each one associated with a different final time T_f and total energy E_t.

Graphically in the criterion space $T_f \times E_t$, the set of all feasible points reveals an area named “Feasible Space” (See Fig. 4). This area is bounded by the set of the optimization results.

An optimal solution is also a Pareto optimal if there is no other solution in the feasible space that reduces at least one objective function without increasing another one [23]. Therefore, in our case, the set of optimal solution is also a Pareto optimal.

Since the trajectory optimization criteria have different quantities (the final time T_f in seconds and the total energy E_t in squared Volts), a normalization parameter becomes necessary. This parameter can be defined as

$$\Lambda = \frac{\Delta E_t}{\Delta T_f}, \tag{45}$$

which gives a “cost ratio”, in J/s.

The optimal solution in the solution set, the Knee Point (T_f^*, E_t^*) is given by:

$$\frac{dE_t(T_f)}{dT_f}(T_f^*) = -\Lambda, \tag{46}$$

Fig. 3 Optimal signals at discrete points i. The arrows indicate signal trend with the increase of penalty parameter μ

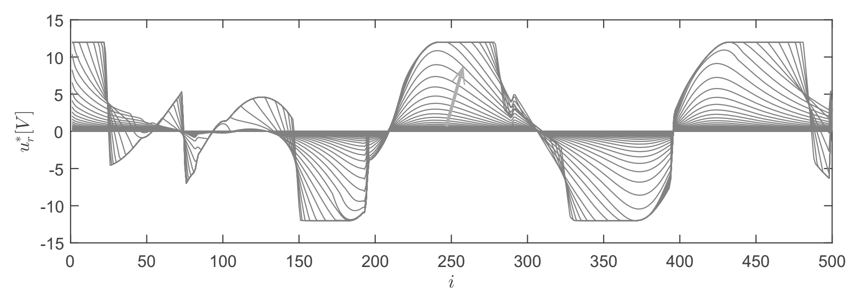

a Optimal input voltage signals u_r^* series

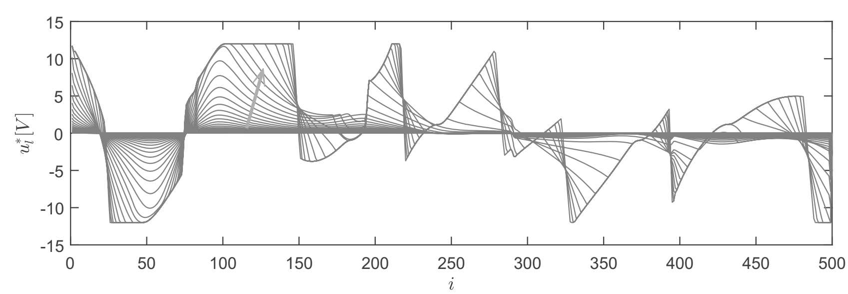

b Optimal input voltage signals u_l^* series

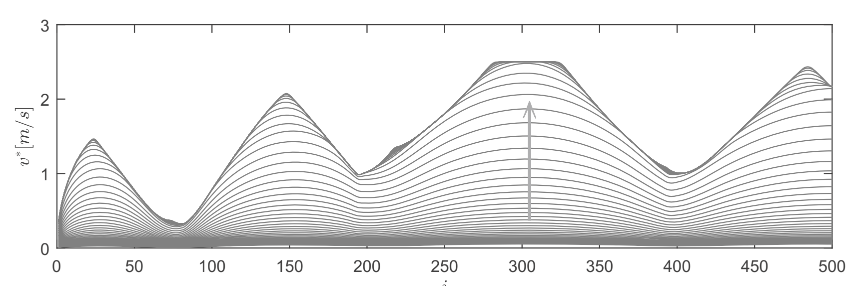

c Optimal velocity profile v^* series

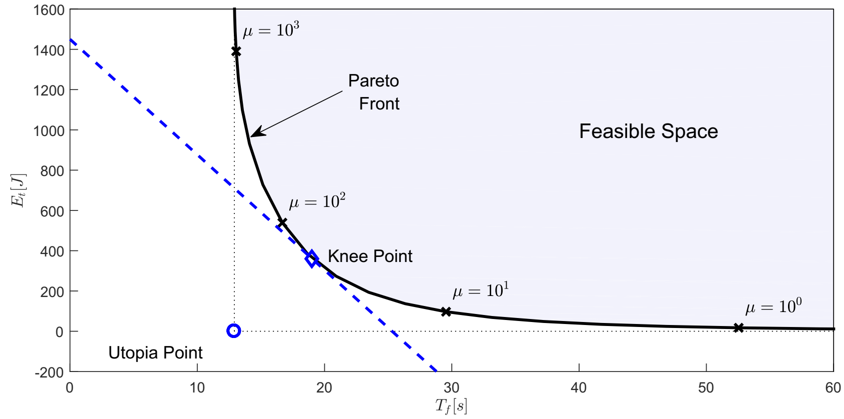

Fig. 4 Criterion space $T_f \times E_t$ with the Utopia and Knee points and the Pareto Front parameterized by the penalty coefficient μ. The dotted lines represent the Pareto Front asymptotes and the dashed line represents a -45^o sloped tangent line through the Knee Point

i.e., the tangent line to the curve on that point in a normalized graph has a slope of -45^o.

3.1 Logarithmic graphs

Experimentally it is possible to note that both the Pareto front graph, Fig. 4, and the $T_f \times \mu$ graph present sections that are linear. These linear sections correspond to regions that are saturation free when plotted in log-log scale as illustrated in Fig. 5. Under these assumptions, it is possible to arguably claim that these functions have an exponential form for some interval values of μ.

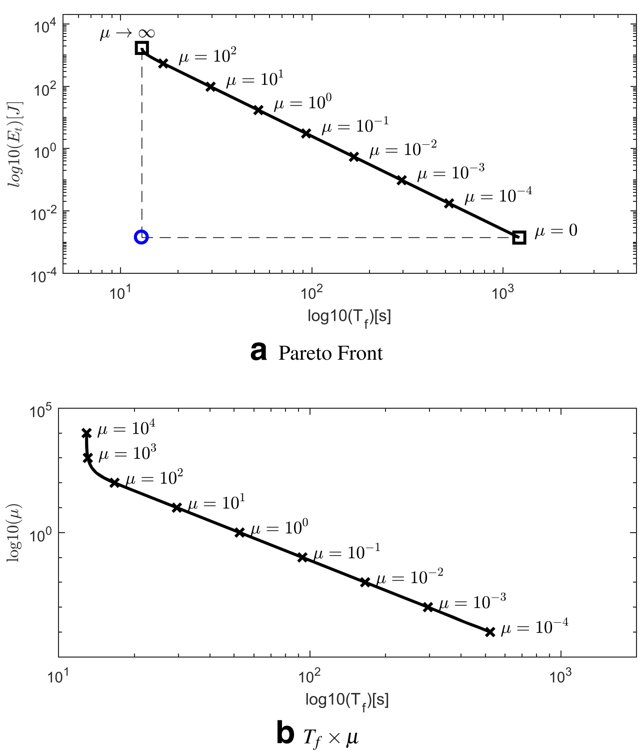

a Pareto Front

b $T_f \times \mu$

Fig. 5 Log-log graphs

4 Self Tuning Algorithm

Suppose that the relationship between the final time T_f and the total energy E_t of the robot in the traversal task is given by the following function:

$$E_t(T_f) = \beta \cdot {T_f}^{\alpha}, \tag{47}$$

where $\alpha, \beta \in \mathbb{R}$ are scalar constants, independent from E_t and T_f. Applying the logarithmic function in Eq. 47 it becomes:

$$\hat{E}_t(\hat{T}_f) = \hat{\beta} + \alpha \cdot \hat{T}_f, \tag{48}$$

where $\hat{(\cdot)} = log10(\cdot)$.

This is an affine function where α is the angular coefficient and $\hat{\beta}$ is the linear coefficient.

Hence, given two different optimization estimates (T_{f1}, E_{t1}) e (T_{f2}, E_{t2}), the α and β coefficients can be calculated by the following equations:

$$\alpha = \frac{\hat{E}_{t2} - \hat{E}_{t1}}{\hat{T}_{f2} - \hat{T}_{f1}}, \tag{49}$$

$$\beta = 10^{(\hat{E}_{t1} - \alpha \hat{T}_{f1})} = 10^{(\hat{E}_{t2} - \alpha \hat{T}_{f2})}. \tag{50}$$

The derivative of Eq. 47 is given by:

$$\frac{dE_t(T_f)}{dT_f} = \alpha\beta \cdot {T_f}^{(\alpha-1)}, \tag{51}$$

such that the tangent line through the Knee Point (T_f^*, E_t^*) has a slope given by the normalization coefficient, Eq. 46, i.e,

$$\alpha\beta \cdot T_f^{*(\alpha-1)} = -\Lambda. \tag{52}$$

Therefore, the Knee Point coordinates is given by:

$$T_f^* = \left(-\frac{\Lambda}{\alpha\beta}\right)^{\frac{1}{(\alpha-1)}}, \tag{53}$$

$$E_t^* = \beta \cdot (T_f^*)^{\alpha}. \tag{54}$$

Table 1 Estimated coefficients α, β, ν and κ for some values of μ

$\hat{\mu}$	T_{f2} $[s]$	E_{t2} $[J]$	$-\alpha$	β $[\times 10^6]$	$-\nu$	κ $[\times 10^6]$
−3	295.46	0.0969	2.9998	2.4979	4.0343	9.2651
−2	166.11	0.5456	2.9999	2.4996	4.0162	8.2725
−1	93.428	3.0662	2.9999	2.4999	4.0112	8.0173
0	52.541	17.241	3.0000	2.5001	4.0085	7.8806
1	29.546	96.949	3.0000	2.5001	4.0068	7.7972
2	16.685	539.17	3.0004	2.5077	4.0106	7.9849
3	13.057	1390.3	3.0578	3.5901	4.3681	7.4839
4	12.910	1674.0	3.0986	4.6356	4.9768	3.3804

Likewise, it is assumed that the relationship between the final time T_f and the penalty coefficient μ is a function $\mu = f(T_f) : \mathbb{R} \rightarrow \mathbb{R}$ given by:

$$\mu(T_f) = \kappa \cdot {T_f}^{\nu}, \tag{55}$$

where $\nu, \kappa \in \mathbb{R}$. Applying the logarithmic function on Eq. 55 it becomes:

$$\hat{\mu}(\hat{T}_f) = \hat{\kappa} + \nu \cdot \hat{T}_f, \tag{56}$$

that is an affine function relating $\hat{T}_f$ to $\hat{\mu}$.

With two optimization points (T_{f1}, μ_1) and (T_{f2}, μ_2), the coefficients ν e κ might be estimated using the following equations:

$$\nu = \frac{\hat{\mu}_2 - \hat{\mu}_1}{\hat{T}_{f2} - \hat{T}_{f1}}, \tag{57}$$

$$\kappa = 10^{(\hat{\mu}_1 - \nu \hat{T}_{f1})} = 10^{(\hat{\mu}_2 - \nu \hat{T}_{f2})}. \tag{58}$$

The complete estimation process is given by Algorithm 1.

Algorithm 1 Estimation of optimal penalty coefficient μ^*

Data: $N, \Gamma, R, M, \mathcal{C}_\tau$
Input: Λ, μ_1, μ_2
Output: μ^*

$(T_{f1}, E_{t1}) \leftarrow SOCP(\mu_1, R, M, \bar{s}'_i, \bar{s}''_i, \mathcal{C}_\tau)$;
$(T_{f2}, E_{t2}) \leftarrow SOCP(\mu_2, R, M, \bar{s}'_i, \bar{s}''_i, \mathcal{C}_\tau)$;
$\alpha \leftarrow (\hat{E}_{t2} - \hat{E}_{t1})/(\hat{T}_{f2} - \hat{T}_{f1})$; `// eq. 49`
$\beta \leftarrow 10^{(\hat{E}_{t1} - \alpha \hat{T}_{f1})}$; `// eq. 50`
$T_f^* \leftarrow (-\Lambda/\alpha\beta)^{(1/(\alpha-1))}$; `// eq. 53`
$E_t^* \leftarrow \beta(T_f^*)^{\alpha}$; `// eq. 54`
$\nu \leftarrow (\hat{\mu}_2 - \hat{\mu}_1)/(\hat{T}_{f2} - \hat{T}_{f1})$; `// eq. 57`
$\kappa \leftarrow 10^{(-\nu \hat{T}_{f1})}$; `// eq. 58`
$\mu^* \leftarrow \kappa(T_f^*)^{\nu}$; `// eq. 55`

5 Results and Discussions

In order to validate the assumption that the relationship between the final time T_f and the total energy E_t is given by an exponential function, numerical results using Algorithm 1 are obtained. For the penalty coefficient value $\mu_1 = 10^{-4}$ the optimization algorithm provides the following solution estimate $(T_{f1}, E_{t1}) = (522.85s, 0.0175J)$. Moreover for each μ^i, $i = -3, \ldots, 4$, the algorithm provides a second solution estimate (T_{f2}, E_{t2}), consequently, the α, β, μ and κ coefficients can be estimated respectively using

Table 2 A comparison between indirect and direct estimation of optimum values

	Algorithm			SOCP		Error
Λ	$T_f^*[s]$	$E_t^*[J]$	μ^*	$T_{fr}^*[s]$	$E_{tr}^*[J]$	$\varepsilon[\%]$
1	52.34	17.44	1.016	52.33	17.45	0.0075
2	44.01	29.34	2.035	44.00	29.38	0.0747
5	35.00	58.33	5.097	34.97	58.48	0.1705
10	29.43	98.10	10.21	29.40	98.46	0.2455
20	24.75	165.0	20.45	24.71	165.8	0.3172
50	19.68	328.0	51.22	19.64	330.1	0.4171
100	16.54	551.7	102.6	16.59	549.1	0.3436
200	13.92	927.8	205.5	14.50	844.0	6.9550
500	11.07	1844.6	514.7	13.36	1182.0	36.5966

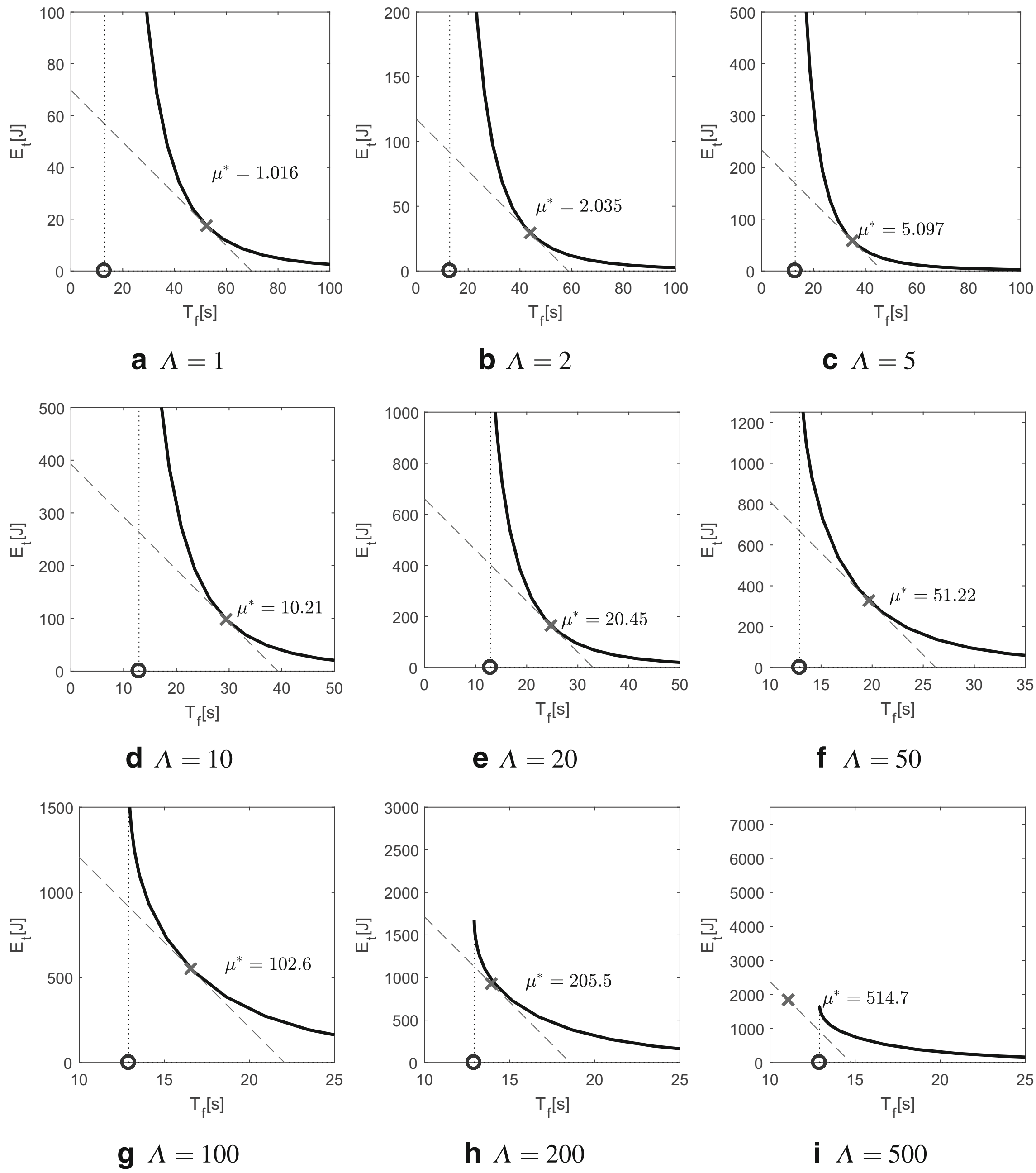

Fig. 6 Criterion spaces $T_f \times E_t$ in some tunning of μ as function of Λ. The red cross indicates the Knee Point (T_f^*, E_t^*) calculated by the Algorithm I and the dashed red line represents the tangent of the Pareto Front at the Knee Point, with a slope of $-\Lambda$

Eqs. 49, 50, 57 and 58. The results of these estimations are illustrated in Table 1.

One can note that there is a linearity in the data especially around $\mu = 10^{-1}$ and $\mu = 10^{1}$. Therefore, the value $\mu_2 = 10^0$ might be arguably used as the second penalty coefficient value for the algorithm.

In order to check our method a two part series of numerical computations are executed. In the first part, where results are named indirect estimation of optimum values, the Algorithm 1 is performed under the assumption that penalty coefficient values $\mu_1 = 10^{-4}$ and $\mu_2 = 10^0$ are sufficient to estimate the parameters of the exponential functions $E_t(T_f)$ and $\mu(T_f)$, respectively (47) and (55).

The following interval range of $\Lambda = [1, 2, 5, 10, 20, 50, 100, 200]$ is considered. The algorithm estimates the optimal solution (T_f^*, E_t^*) as the estimated optimal point and the associated penalty coefficient μ^*. These results are illustrated in the left part of Table 2.

In the second part, where results are named direct estimation of optimum values, the SOCP (Problem 4)

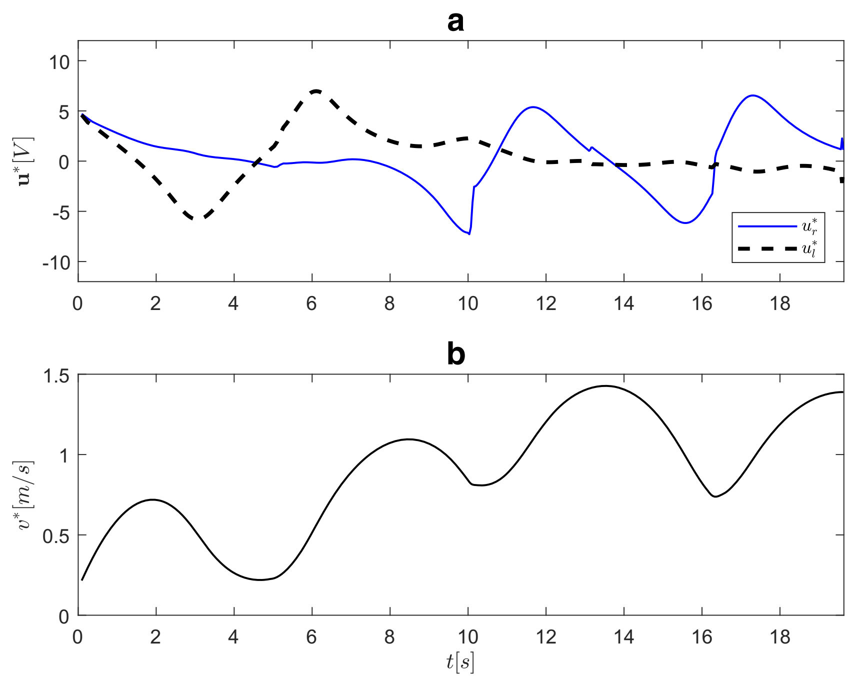

Fig. 7 Optimum signals from SOCP for $\mu^* = 51.22$

optimization algorithm is executed for each value of Λ with the associated optimal penalty coefficient μ^* estimated in the first part. The algorithm estimates optimal points (T_{fr}^*, E_{tr}^*) that are illustrated in the right part of the Table 2.

In the right part of the Table 2 the mean relative errors of indirect and direct estimation of optimum values are calculated for each Λ as follows:

$$\varepsilon = \frac{|T_{fr}^* - T_f^*|/T_{fr}^* + |E_{tr}^* - E_t^*|/E_{tr}^*}{2} \times 100. \tag{59}$$

Graphical results are illustrated in Fig. 6. It is possible to note that on case (h), where $\Lambda = 200$ the estimated optimal point is almost close to the edge of saturation. Since the mean relative error is greater than 1%, normalization coefficient values $\Lambda \gg 100$ should be avoided.

The generation of voltage signals profiles are the final goal of the optimization algorithm. Fig. 7 illustrates (a) optimal voltage signals $u^*(t) = [\, u_r^*(t) \;\; u_l^*(t)\,]^T$ that drives the robot along the geometric path Γ (See Fig. 2) and (b) optimal velocity profile $v^*(t)$, for a normalized coefficient value $\Lambda = 50$ (penalty coefficient $\mu^* = 51.22$).

6 Conclusions

A method for trajectory planning based on time-energy optimization of a nonholonomic wheeled mobile robot has been proposed. A nonlinear variable change allows the transformation of a nonlinear optimization problem into a discrete second order cone programming that can be solved by convex optimization tools. An alternative generalized coordinate system is used by considering that the predetermined geometric path is a constraint.

The convex optimization algorithm estimates a solution (T_f, E_t) which is a function of the penalty coefficient μ. The function is drawn as a curve in the criterion space $T_f \times E_t$ parameterized by the penalty coefficient μ. The curve might also be interpreted as a Pareto Front. There is a special interest in estimating the Knee Point that is an optimal solution that balances equally the traversal time and total energy.

The main rationale of this work hypothesize that both functions $E_f(T_f)$ and $T_f(\mu)$ are exponentially shaped. When Estimating two solutions of the curve (T_f, E_t) it is possible to estimate the parameters of the exponential functions and infer the value of the optimal penalty coefficient μ^* which is associated to the Knee Point.

Using the value of μ^* it is possible to estimate the optimal solution (T_f^*, E_t^*) and consequently the associated optimal voltage signals $u^*(t) = [\, u_r^*(t) \;\; u_l^*(t)\,]^T$.

Using numerical results, optimal values (T_f^*, E_t^*) are estimated using two different methods: indirect and direct estimation. The obtained small mean relative errors that is used to compare both estimations demonstrates the feasibility of the method.

This systematic approach might be understood as a self-tuning algorithm that estimate the penalty coefficient for the generation of optimal voltage signals.

References

1. Liu, S., Sun D.: Minimizing energy consumption of wheeled mobile robots via optimal motion planning. IEEE Trans. Mechatron. **19**(2), 401–411 (2014)
2. Kim, H., Kim, B.K.: Minimum-Energy Translational Trajectory Plan- Ning for Battery-Powered Three-Wheeled Omni-Directional Mobile Robots. In: Proceedings IEEE International Conference Control, Autom., Robot. Vis., 1730–1735 (2008)
3. Mei, Y., Lu, Y., Lee, C., Hu, Y.: Energy-Efficient Mobile Robot Exploration. In: IEEE International Conference Robot. Autom., 505–5011 (2006)
4. Hsu, D., Kindel, R., Latombe, J., Rock, S.: Randomized kinodynamic motion planning with moving obstacles. Int. J. Rob. Res. **21**(3), 233–255 (2002)
5. Pham, Q., CAron, S., Nakamura, Y.: Kinodynamic Planning in the Configuration Space via Velocity Interval Propagation. In: Robotics: Science and Systems (2006)
6. LaValle, S.: Planning Algorithms. Cambridge University Press, New York (2006)
7. Bobrow, J.E., Dubowsky, S., Gibson, J.S.: Time-Optimal Control of robotic manipulators along specified paths. Int. J. Robot. Res. **4**, 3–17 (1985)
8. Pfeiffer, F., Johanni, R.: A concept for manipulator trajectory planning. IEEE J. Robot. Autom. **3**(2), 115–123 (1987)
9. Shiller, Z.: Time-Energy Optimal control of articulated systems with geometric path constraints. J. Dyn. Syst. Meas. Control. **118**(1), 139–143 (1996)
10. Constantinescu, D., Croft, E.A.: Smooth and time-optimal trajectory planning for industrial manipulators along specified paths. J. Robot. Syst. **17**(5), 233–249 (2000)
11. Verscheure, D., Demeulenaere, B., Swevers, J., De Schutter, J., Diehl, M.: Time-energy optimal path tracking for robots: a numerically efficient optimization approach. In: Proceedings of the 10th IEEE International Workshop on Advanced Motion Control, 727–732 (2008)
12. Verscheure, D., Demeulenaere, B., Swevers, J., De Schutter, J., Diehl, M.: Time-optimal path tracking for robots: a convex optimization approach. IEEE Trans. Autom. Control **54**(10), 2318–2327 (2009)
13. Boyd, S.P., Vandenberghe, L.: Convex Optimization. Cambridge University Press, Los Angeles (2004)
14. Ardeshiri, T., Norrlöf, M., Löfberg, J., Hansson, A.: Convex optimization approach for Time-Optimal path tracking of robots with speed dependent constraints. In: Proceedings of the 18th IFAC World Congress, 44(1), 14648–14653 (2011)
15. Debrouwere, F., Van Loock, W., Pipeleers, G., Dinh, Q.T., Diehl, M., De Schutter, J., Swevers, J.: Time-Optimal Path following for robots with convex - concave constraints using sequential convex programming. IEEE Trans. Robot. **29**(6), 1485–1495 (2013)
16. Zhang, Q., Li, S.-R., Gao, X.-S.: Practical smooth minimum time trajectory planning for path following robotic manipulators. In: Proceedings of the 2013 American Control Conference, 2778–2783 (2013)
17. Lipp, T., Boyd, S.: Minimum-time speed optimisation over a fixed path International Journal of Control, 87(6), 1297–1311 (2014)
18. Reynoso-Mora, P., Chen, W., Tomizuka, M.: A convex relaxation for the time-optimal trajectory planning of robotic manipulators along predetermined geometric paths. Optimal Control Appl. Methods **37**(6), 1263–1281 (2016)
19. Siciliano, B., Khatib, O. (eds.): Springer handbook of robotics. Springer, Berlin (2008)
20. Serralheiro, W., Maruyama, N.: Time-Energy Optimal trajectory planning over a fixed path for a wheeled mobile robot. In: Proceedings of the 14th International Conference on Informatics in Control, Automation and Robotics, 239–246 (2017)
21. Lobo, M.S., Vandenberghe, L., Boyd, S., Lebret, H.: Applications of second-order cone programming. Linear Algebra Appl. **284**(1–3), 193–228 (1998)
22. Grant, M., Boyd, S.: CVX: MATLAB Software for Disciplined Convex Programming, version 2.1. http://cvxr.com/cvx,. Accessed 12 May 2017 (2014)
23. Arora, J.S.: Introduction to optimum design. Elsevier, Oxford (2012)

Werther Serralheiro received the B.Eng. degree in Control and Automation Engineering (1998) and the M.Eng. degree in Production Engineering (2004), both from the Federal University of Santa Catarina, Brazil, and the Ph.D. degree in Mechanical Engineering (2018) from Polytechnic School of the University of São Paulo. He is since 2007 a professor in Department of Electromechanics at Federal Institute of Santa Catarina. Werther's research interest are focused on control systems, mobile robotics, convex optimization and its application in mechatronics.

Fabrício Saggin received in 2013 the B.Eng. degree in Electrical and Automation Engineering from ENSEEIHT, France. He received the B.Eng. degree in Electrical Engineering (2013) and the M.Eng. degree in Automation and Systems Engineering (2016), both from the Federal University of Santa Catarina, Brazil. He is currently working towards the Ph.D. degree in the Ecole Centrale de Lyon. His research interests are control systems, droop control and synchronous power systems.

Newton Maruyama received the B.Eng. degree in Electrical Engineering (1987) and the M.Eng. degree in Mechatronics Engineering (1991) from the Polytechnic School of the University of São Paulo, Brazil. In 1997, he received the D.Phil. degree in Engineering Science from the University of Oxford, United Kingdom. Newton is since 1997 a professor in the Department of Mechatronics Engineering and Mechanical Systems at Polytechnic School of the University of São Paulo. His main research interests include control systems, autonomous robots, embedded systems, and real-time systems control architecture.